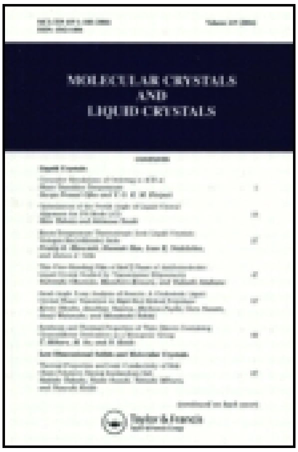

Molecular Crystals and Liquid Crystals
Publication details, including instructions for authors and subscription information:
http://www.tandfonline.com/loi/gmcl20

Study of Critical Behaviour of the Thermal Parameters in the Phase Transition in Mesogenic Materials

V. Bruno [a], N. Scaramuzza [a] & U. Zammit [b]

[a] Dipartimento di Fisica, dell'Università della Calabria and Sezione INFM "della Calabria", Arcavacata di Rende (Cosenza), I-87036, Italy

[b] Dipartimento di Ingegneria Meccanica, Università di Roma and Sezione INFM "Tor Vergata", Via di Tor Vergata 110, Roma, 00133, Italy

Version of record first published: 29 Oct 2010

To cite this article: V. Bruno, N. Scaramuzza & U. Zammit (2002): Study of Critical Behaviour of the Thermal Parameters in the Phase Transition in Mesogenic Materials, Molecular Crystals and Liquid Crystals, 372:1, 201-215

To link to this article: http://dx.doi.org/10.1080/10587250127579

Mol. Cryst. and Liq. Cryst., 2001, Vol. 372, pp. 201-215

Study of Critical Behaviour of the Thermal Parameters in the Phase Transition in Mesogenic Materials

V. BRUNO[a]*, N. SCARAMUZZA[a] and U. ZAMMIT[b]

[a]*Dipartimento di Fisica dell'Università della Calabria and Sezione INFM "della Calabria", I-87036 Arcavacata di Rende (Cosenza), Italy and*
[b]*Dipartimento di Ingegneria Meccanica, Università di Roma and Sezione INFM "Tor Vergata", Via di Tor Vergata 110, 00133 Roma, Italy*
**Author for correspondence*

Abstract The photopyroelectric technique has been adopted to study the critical behaviour associated with the thermal parameters over smectic A – nematic (S_A-N) phase transition in both *4-n-nonyl-4'-cyanobiphenyl* (9CB) and *4-n-pentylphenylthiol-4'-n-octyloxythiolbenzoate* ($\overline{8}$S5) through the simultaneous determination of the specific heat (*c*) as well as of transport parameters like thermal diffusivity (*D*) and thermal conductivity (*k*). In the case of 9CB, the critical exponent of specific heat agrees with the value of 0.5 expected from the theory of mean field tricritical behaviour. On the other hand, for $\overline{8}$S5 the values of critical exponent is close to the one of 3D XY-like second order phase transition, in agreement with earlier investigations. In all cases the thermal conductivity showed no anomaly.

Keywords: Thermal parameters; Phase transition; Photopyroelectric technique; Liquid Crystals

INTRODUCTION

The measurements of thermal transport parameters in liquid crystals has attracted considerable attention, using a variety of techniques, [1-11]. Among the adopted techniques, photothermal techniques [7-11] have been developed in the last years and have enabled the study the critical behaviour of transport thermal parameters [9,11]. Such techniques are based on the effect of the periodic heating of a sample by a modulated laser source and, due to its peculiar characteristics, they are used in many research fields like medicine, biology, engineering, and study of new materials [12]. In general the critical behaviour of thermal parameters near phase transitions presents some anomaly like a divergence or dip, where a strong dependence of parameters on temperature is present. To correctly study such dependence, without changing its behaviour as a function of temperature, a low perturbative technique is required, that is small thermal gradients induced in the sample at the equilibrium. This allows high temperature resolution of critical behaviour of thermal parameters. Furthermore the photothermal techniques are useful because allows simultaneous measurements of specific heat (c) as well as transport parameters like thermal diffusivity (D) and thermal conductivity (k). Therefore it is possible to study static and dynamic critical behaviour at phase transition with the same measurement for a complete characterisation of the material under study.

A calorimetric system based on the photopyroelectric technique has been used to study phase transitions in thermotropic liquid crystals. In particular the critical behaviour at smectic A – nematic (S_A-N) transition in samples of *4-n-nonyl-4'-cyanobiphenyl* (9CB) and *4-n-pentylphenylthiol-4'-n-octyloxythiolbenzoate* ($\overline{8}S5$) has been studied and the critical exponents of *c*, *D* and *k* has been measured.

The transition S_A-N can be both first or second order and, on the basis of a mean-field theory, Kobayashi [13] and McMillan [14] have shown that the transition should be second order if the ratio $T_{AN}/T_{NI}<0.87$ (T_{AN} and T_{NI} being the S_A-N and nematic-isotropic transition temperatures). The theory predict the existence of a tricritical point (TCP) for $T_{AN}/T_{NI}=0.87$, where the transition switches from first to second order. In particular, it has been shown that in compounds where the McMillan ratio T_{AN}/T_{NI} is less than 0.93, the critical behaviour of *c* can be described by the isotropic three-dimensional (3D) XY model which predicts the critical exponent $\alpha = -0.007$ [15]. Furthermore, the TCP was experimentally observed at the S_A-N transition in several compounds and a mean-field tricritical value $\alpha = 0.5$ observed [16].

THEORETICAL FRAMEWORK

The photopyroelectric effect is based on the use of a pyroelectric transducer to detect the temperature rise of a light induced periodic heating of a sample. The temperature variation in the transducer gives rise to an electrical current proportional to the rate of change of its average heat content. The theory describing the photopyroelectric effect has been developed by A. Mandelis and M. Zver [17]. It consist in an unidimensional model that connect the signal output of the pyroelectric transducer with the values of the optical and thermal parameters of the material under examination placed in contact with pyroelectric element.

The pyroelectric element is represented by an ideal current source with a parallel leakage resistance R_p and a capacitance C_p, while the detection electronics is described by an input capacitance C_d and a parallel load resistance R_d [18].

From the analysis of the equivalent circuit and neglecting the effect of the transmission line between the sensor and the electronic, the signal output is given by

$$V(\omega) = \frac{APR\,j\omega}{1 + j\omega\tau_e}\theta_p(\omega) \qquad (\text{or } V(\omega) \propto \theta_p(\omega)) \qquad (1)$$

where $\theta_p(\omega)$ represent the complex amplitude of the temperature oscillations in the pyroelectric transducer, integrated over its thickness at the angular frequency ω, A is the area of the pyroelectric element, P is the pyroelectric coefficient of the transducer, and $\tau_e = RC$ with $R = R_d R_p/(R_d + R_p)$ and $C = C_d + C_p$.

The $\theta_p(\omega)$ is obtained by resolving the equations of the thermal diffusion through the four different media composing the system (fig.1).

The obtained solution can be simplified assuming that both the sample and the pyroelectric transducer are optically opaque and thermally thick. [18].

A medium is optically opaque when the optical absorption length $\mu_\beta = 1/\beta < l$, where β is the optical absorption coefficient and l the medium thickness. On the other hand, a medium is thermally thick when the thermal diffusion length $\mu = \sqrt{\frac{2D}{\omega}} < l$, where $D = k / c\rho$ is the thermal diffusivity, k the thermal conductivity, c the specific heat and ρ the density.

With these assumptions, the amplitude and the phase of the pyroelectric signal are, respectively [18]:

$$|V(\omega)| = \frac{I_0 \eta_s APR}{l_p \rho_p c_p \sqrt{1+\omega^2 \tau_e^2}} \times \frac{e_p e^{-\sqrt{\frac{\omega}{2D_s}}\, l_s}}{e_s \left(1+e_g / e_s\right)\left(1+e_p / e_s\right)} \tag{2}$$

$$\phi(\omega) = -\tan^{-1}(\omega \tau_e) - \sqrt{\frac{\omega}{2D_s}}\, l_s \tag{3}$$

being I_0 the intensity of the non reflected part of the incident radiation, η the sample nonradiative conversion efficiency, $e = \sqrt{\rho\, ck}$ the thermal effusivity. The subscript s, p and g refer to the sample, pyroelectric transducer and medium in contact with the sample front surface respectively.

Generally, the critical behaviour of the specific heat is described by a function of the form [9]:

$$c_s = B + E\,t + A^{\pm}|t|^{-\alpha}(1 + D^{\pm}|t|^{0.5}) \tag{4}$$

and when the thermal conductivity shows no anomaly as in the present case [9],

$$k_s = \rho\,(H + G\,t) \tag{5}$$

$$D_S = \frac{H + G(T - T_c)}{B + E\,t + A^{\pm}|t|^{-\alpha}(1 + D^{\pm}|t|^{0.5})} \tag{6}$$

where B, E, H, G, $A^{\pm}$ and $D^{\pm}$ are adjustable parameters and $\pm$ indicates, respectively, values relative to data above and below T_{AN}.

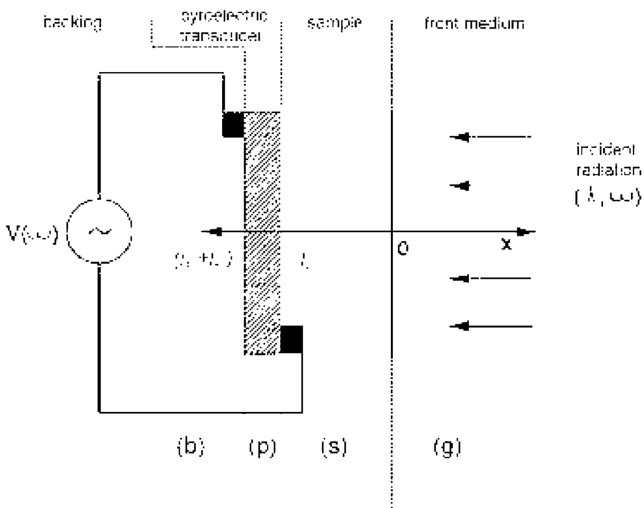

FIGURE 1 Schema of photopyroelectric detection.

EXPERIMENTAL SET-UP

In figure 2 is shown the diagram of the experimental set-up used to study the behaviour of static and dynamic thermal parameters of liquid crystal samples.

The sample cell (fig. 3) was contained in a cylindrical oven that was uniformly heated on the outer lateral surface. The temperature was measured by a thermistor that was as close as possible to the sample and the heating rate was computer controlled via a current supply. The heating light was supplied by a He-Ne laser operating at 633 nm, acousto-optically modulated. The subsequent pyroelectric signal was revealed by a lock-in amplifier and data acquired by the computer.

The cell has been coated on the surface in contact with the sample, where the light is incident, with an optically thick gold film. The film thickness was ~0.5 μm and thermally thin at the modulation frequency used (77 Hz). The metal film ensured that the condition of sample optically opaque $1/\beta_s \ll l_s$. The pyroelectric transducer is a 300 μm thick $LiTaO_3$ single crystal and acts also as a cover for the cell. It can be used in a wide temperature range, from few tens of K to its Curie point (~600°C) and presents a relatively high sensitivity (2.2 ~$2.5*10^{-8}$ C cm^{-2} K^{-1} [19]). Being the $LiTaO_3$ a dielectric, both sides have been coated with transparent ITO (indium tin oxide) electrodes. Using ITO electrodes allowed checking the sample at microscope once closed the cell.

During high resolution measurements performed using this experimental set-up it's important to reduce the effects of thermal gradients that could be introduced by too fast a heating rate or too large a light power density. The heating rate was <1 mK/min and the laser light power density have been reduced to less than 1 mW/cm^2 . The use of a lock-in amplifier allowed an acceptable noise to signal ratio with a pyroelectric signal of few μV.

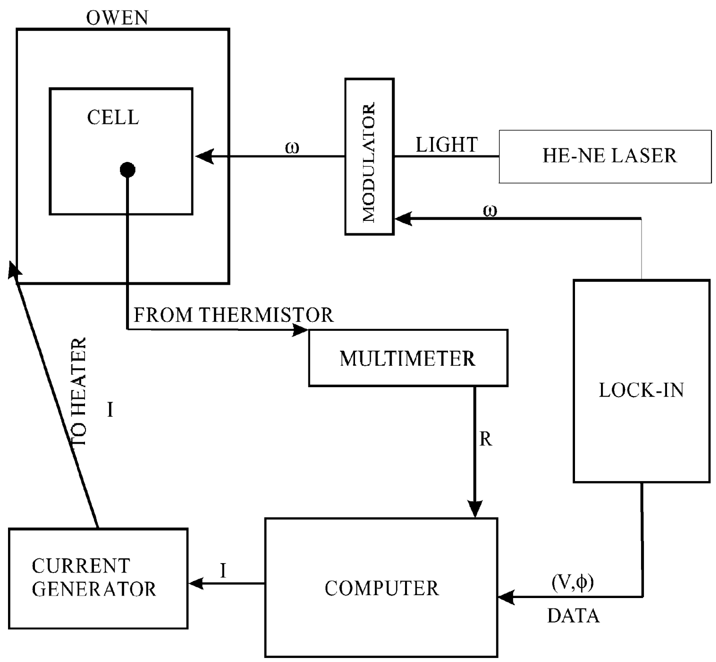

FIGURE 2 Experimental set-up

RESULTS AND DISCUSSION

To test the experimental set-up, we performed measurements of specific heat (*c*), the thermal diffusivity (*D*) and the thermal conductivity (*k*) on 9CB material which behaviour to the phase transition S_A-N is reported in literature [20]. In figs. 4 are reported the phase and amplitude behaviours for 9CB material, of the signal obtained by the experimental set-up

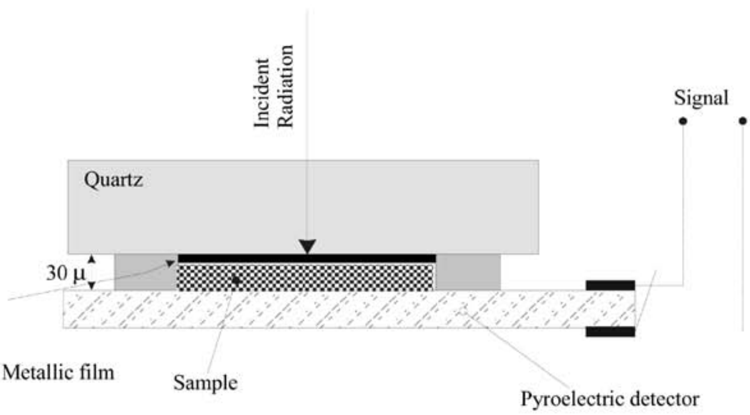

FIGURE 3 Photoelectric cell for liquid crystal samples

previously described. From the figures is evident that the 9CB presents both a phase transition S_A-N at the temperature T_{AN}=47.7 °C and a phase transition nematic – isotropic (N-I) at the temperature T_{NI}=49.7 °C. In this case the McMillan ratio is $T_{AN}/T_{NI} = 0.994$.

High resolution measurements have been performed to obtain the critical exponents of thermal parameters at the transition S_A-N. In figs. 5 are reported the specific heat, the thermal diffusivity and the thermal conductivity critical behaviour for 9CB vs. the reduced temperature $t=(T-T_{AN})/T_{AN}$. The full lines represent the best fits obtained by means the eqs. 4-6.

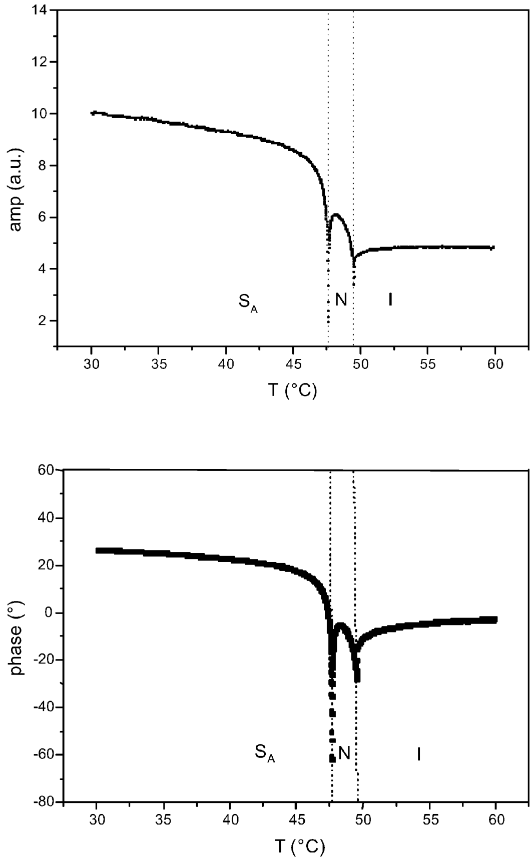

FIGURE 4 Photopyroelectric signal amplitude and phase vs. temperature for 9CB liquid crystal

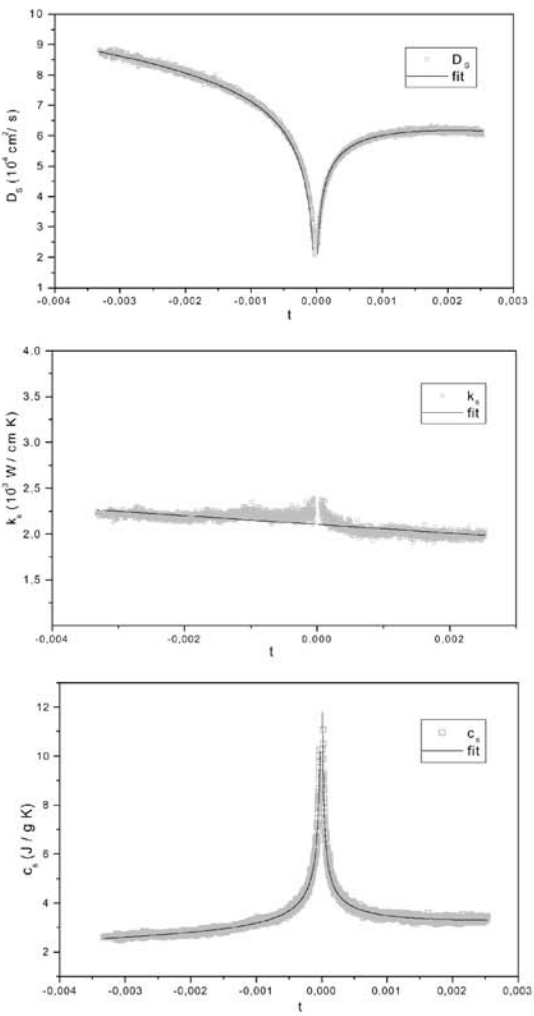

FIGURE 5 (a) Thermal diffusivity behaviour vs. reduced temperature t of 9CB liquid crystal at the smectic A-Nematic phase transition; (b) Thermal conductivity behaviour vs. reduced temperature t of 9CB liquid crystal at the smectic A-Nematic phase transition; (c) specific heat behaviour vs. reduced temperature t of 9CB liquid crystal at the smectic A-Nematic phase transition. The full lines represent the best fits obtained by means the eqs. 4-6.

In Table 1 are reported the values of critical exponents obtained by means the best fits performed on the experimental data of specific heat and thermal diffusivity. They are very close to the value of 0.5 expected from the theory [21].

The other material investigated was the $\overline{8}S5$. It has a wide nematic range (~ 23 °C), so that the critical behaviour of thermal parameters, because of the small influence of N-I transition on S_A-N ones, should be close to that expected form the 3D XY model [21].

	9CB	$\overline{8}S5$
c	**0.56±0.03**	**-0.024±0.009**
D	**0.57±0.03**	**-0.027±0.011**

TABLE 1 Values of critical exponents for 9CB and $\overline{8}S5$, respectively

In figs 6 are reported the high resolution measurements of the specific heat, the thermal diffusivity and the thermal conductivity for the $\overline{8}S5$ material. The full lines represent the best fits obtained by means the eqs. 4-6. The values of critical exponents obtained by means the best fits performed on the experimental data of specific heat and

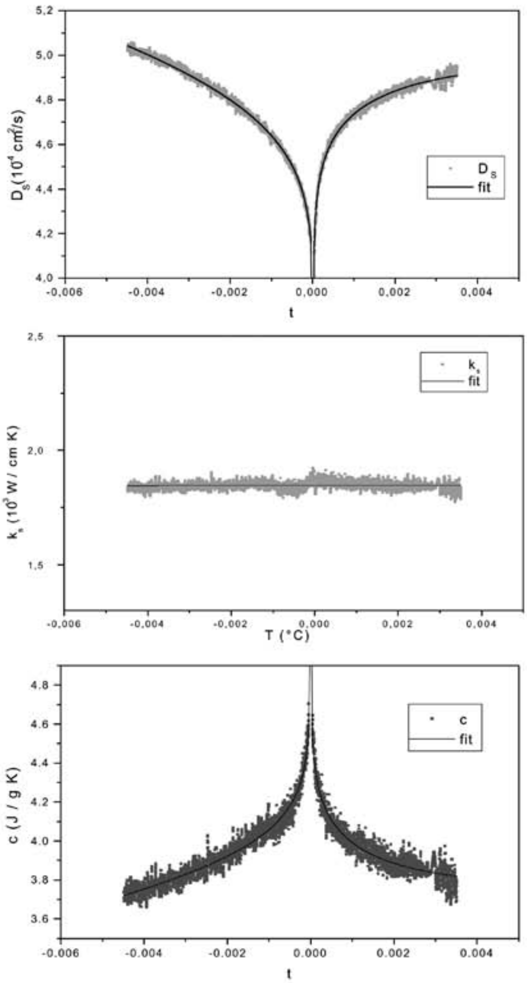

FIGURE 6 (a) Thermal diffusivity behaviour vs. reduced temperature t of $\overline{8}$S5 liquid crystal at the smectic A-Nematic phase transition; (b) Thermal conductivity behaviour vs. reduced temperature t of $\overline{8}$S5 liquid crystal at the smectic A-Nematic phase transition; (c) specific heat behaviour vs. reduced temperature t of $\overline{8}$S5 liquid crystal at the smectic A-Nematic phase transition. The full lines represent the best fits obtained by means the eqs. 4-6.

thermal diffusivity are reported in Table 1. It is interesting to note that the values of critical exponents obtained in this case are more similar with the one of 3D XY-like second order phase transition (-0.007) [21].

CONCLUSION

Simultaneous measurements of thermal diffusivity, thermal conductivity and specific heat in 9CB and $\overline{8}$S5 samples have been reported. High resolution measurements have been performed to obtain the critical exponents of thermal parameters at the transition S_A-N. In the case of 9CB, the critical exponent of specific heat agrees with the value of 0.5 expected from the theory. On the other hand, for $\overline{8}$S5 the values of critical exponent is close with the one of 3D XY-like second order phase transition.

Aknowledgements

The authors wish to thank Dr. F. Mercuri and Prof. M. Marinelli for their invaluable help in setting up the experimental technique and are indebted to Prof. R. Bartolino for the fruitful discussion and the helpful suggestions.

References

1) W. Urbach, H. Hervet and F. Rondelez, J. Chem. Phys. **78,** 5113 (1983).
2) R. Vilanove, E. Guyon, C. Mitescu, and P. Pieranski, J. Phys. (Paris) **35,** 153 (1974).

3) W. Urbach, H. Hervet and F. Rondelez, Mol. Cryst. Liq. Cryst. **46,** 409 (1978).
4) F. Rondelez, W. Urbach, and H. Hervet, Phys. Rev. Lett. **41,** 1058 (1978).
5) T. Akahane, M. Kondoh, K. Hashimoto, and M. Nakagawa, Jpn. J. Appl. Phys. **26,** L1000 (1987).
6) G. Ahlers, D.S. Cannel, L.I. Berge, and S. Sakurai, Phys. Rev. E **49,** 545 (1984).
7) Y.G. Fuh and R.F. Code, Can. J. Phys. **63,** 282 (1985).
8) A.C. Bento, A.J. Palgana, L.R. Evangelista, M.L. Baesso, J.R.D. Pereira, E.C. da Silva, and A.M. Mansanares, Appl. Phys. Lett. **68,** 3371 (1996).
9) M. Marinelli, F. Mercuri, S. Foglietta, U. Zammit, and F. Scudieri, Phys. Rev. E **54,** 1604 (1996).
10) J. Caerels, E. Schoubs, and J. Thoen, Liq. Cryst **22,** 659 (1997).
11) F. Mercuri, U. Zammit, and M. Marinelli, Phys. Rev. E **57,** 596 (1998).
12) L.P. Kadanoff, Rev. Mod. Phys. **39**, 395 (1967).
13) K.K. Kobayashi, Mol. Cryst. Liq. Cryst. **13**, 137 (1971).
14) L. McMillan, Phys. Rev. A **4**,1238 (1971).
15) C.W. Garland, G. Nounesis, and K.J. Stine, Phys. Rev. A **39**, 4919 (1989).
16) M.A. Anisimov, Mol. Cryst. Liq. Cryst. **162A**, 1 (1988).
17) A. Mandelis and M. Zver, J. Appl. Phys. 57, 4421 (1985).
18) M. Marinelli, U. Zammit, F. Mercuri, and R. Pizzoferrato, J. Appl. Phys. **72(3)**, 1096 (1992).
19) P. Beerman, Infrared Physics, **15**, 225 (1975).
20) M. Marinelli, F. Mercuri, U. Zammit, and F. Scudieri, Phys. Rev. E **58**, 5860 (1998).
21) C. Bervillier, Phys. Rev. B **34**, 8141 (1986); T.C. Lubeski, J. Chem. Phys., **80**, 31 (1983).